PROCEEDINGS B

royalsocietypublishing.org/journal/rspb

Natural selection on a carbon cycling trait drives ecosystem engineering by *Sphagnum* (peat moss)

Bryan T. Piatkowski[1], Joseph B. Yavitt[2], Merritt R. Turetsky[3] and A. Jonathan Shaw[1]

[1]Department of Biology, Duke University, Durham, NC 27708, USA
[2]Department of Natural Resources, Cornell University, Ithaca, NY 14853, USA
[3]Institute of Arctic and Alpine Research, University of Colorado, Boulder, CO 80309, USA

BTP, 0000-0002-1334-8431; JBY, 0000-0002-8292-7824; MRT, 0000-0003-0155-8666; AJS, 0000-0002-7344-9955

Research

Cite this article: Piatkowski BT, Yavitt JB, Turetsky MR, Shaw AJ. 2021 Natural selection on a carbon cycling trait drives ecosystem engineering by *Sphagnum* (peat moss). *Proc. R. Soc. B* **288**: 20210609.
https://doi.org/10.1098/rspb.2021.0609

Received: 11 March 2021
Accepted: 26 July 2021

Subject Category:
Evolution

Subject Areas:
evolution, ecology, plant science

Keywords:
extended phenotype, *Sphagnum*, litter decomposition, niche construction, ecosystem engineer, carbon cycle

Author for correspondence:
Bryan T. Piatkowski
e-mail: piatkowskibt@ornl.gov

Electronic supplementary material is available online at https://doi.org/10.6084/m9.figshare.c.5542663.

THE ROYAL SOCIETY
PUBLISHING

Sphagnum peat mosses have an extraordinary impact on the global carbon cycle as they control long-term carbon sequestration in boreal peatland ecosystems. *Sphagnum* species engineer peatlands, which harbour roughly a quarter of all terrestrial carbon, through peat accumulation by constructing their own niche that allows them to outcompete other plants. Interspecific variation in peat production, largely resulting from differences in tissue decomposability, is hypothesized to drive niche differentiation along microhabitat gradients thereby alleviating competitive pressure. However, little empirical evidence exists for the role of selection in the creation and maintenance of such gradients. In order to document how niche construction and differentiation evolved in *Sphagnum*, we quantified decomposability for 54 species under natural conditions and used phylogenetic comparative methods to model the evolution of this carbon cycling trait. We show that decomposability tracks the phylogenetic diversification of peat mosses, that natural selection favours different levels of decomposability corresponding to optimum niche and that divergence in this trait occurred early in the evolution of the genus prior to the divergence of most extant species. Our results demonstrate the evolution of ecosystem engineering via natural selection on an extended phenotype, of a fundamental ecosystem process, and one of the Earth's largest soil carbon pools.

1. Introduction

Sphagnum is arguably the most important plant genus for terrestrial carbon storage worldwide. These mosses both create and dominate boreal peatland ecosystems through their ability to sequester huge amounts of carbon in peat soil that forms when rates of growth surpass those of decomposition [1–3]. Indeed, it is likely that more carbon is bound in living and dead *Sphagnum* than in any other genus of plants [4]. Consequentially, this genus has a profound influence on global climate despite the relatively recent diversification of most extant species, perhaps 7–20 Ma during a period of climatic cooling in the Northern Hemisphere [5].

Peat formation is facilitated by the production of plant tissue that decomposes slowly in the water-logged, acidic and nutrient-poor conditions of peatlands, which give these mosses a competitive edge over other plants [6,7]. However, a prominent feature among many *Sphagnum* species is their height-above-water-table niche thought to result from interspecific differences in rates of peat accumulation. Some species form hummocks elevated up to a metre above the surrounding water table, whereas others live in hollows at or near the water table [8,9]. This niche differentiation can result in the coexistence of 20 or more species of *Sphagnum* within peatlands by alleviating the ecological pressures associated with competition among congenerics.

Our understanding about the evolution of *Sphagnum* species having such different rates of tissue decay is incomplete. Early comparative studies of *Sphagnum* found that hummock-forming species both grow and decay more slowly than hollow-dwelling species [10,11]. Reciprocal transplant experiments showed these differences occurred regardless of the microhabitat in which the experiment was conducted and decay generally occurred faster in the hummock microhabitat [12,13], suggesting that differences in decomposability among species are not caused primarily by environmental factors. Recent studies have expanded the number of *Sphagnum* species sampled and biochemical correlates associated with such processes [14–16], showing that hummock-forming species tend to have higher amounts of structural carbohydrates and lignin-like phenolics in their cell walls. For some of these metabolites, variation is influenced by environmental conditions (e.g. the water-soluble phenolics studied by [17]) in addition to having strong genetic components. Nevertheless, low decomposability is an emergent property of litter biochemistry that results in the creation and maintenance of hummocks.

However, it is unclear how natural selection impacted the evolution of tissue decomposability despite the oft-quoted tenet that peat accumulation is adaptive for *Sphagnum*. Empirical studies have demonstrated that interspecific variation in height-above-water-table (i.e. formation of hummocks), and some of the functional traits hypothesized to underlie position along this hydrological gradient are phylogenetically conserved [18,19]. Various measures of growth, decomposability and litter biochemistry show evolutionary covariance with height-above-water-table and might represent adaptive syndromes in *Sphagnum* related to niche [19]. Such syndromes of covarying traits are hallmarks of natural selection [20,21] but the evolutionary mechanisms by which these traits evolved in *Sphagnum* remain largely unknown. Furthermore, only laboratory-based measurements of decomposition rate in previous studies had detectable phylogenetic signal, and it is unknown if such patterns of interspecific variation are realized under natural conditions.

Therefore, we quantified variation in biomass decomposability for 54 species to understand how this trait evolved during *Sphagnum* diversification. We competed phylogenetic models of trait evolution that varied in the degree to which natural selection explained patterns of interspecific variation and in the heterogeneity of evolutionary forces across lineages. We hypothesized that selection favours different levels of decomposability corresponding to different microhabitat preferences, and that decomposability coevolved with realized niche along the hydrological height-above-water-table gradient in response to natural selection. These analyses provide an opportunity to link plant traits to niche differentiation within communities and to link such niche differentiation to global scale carbon sequestration.

2. Material and methods

(a) Study species

We sampled 54 *Sphagnum* species that spanned the phylogenetic breadth of the genus, representing the majority of those species distributed in North America. Our sampling came from a total of 198 collections and 48 localities throughout North America. On average, each locality had 3.7 different species present, and each species was found at 3.3 different localities. Previous phylogenetic analyses of *Sphagnum* used full organellar genome sequences and resolved five subgenera: *Rigida*, *Sphagnum*, *Acutifolia*, *Cuspidata* and *Subsecunda* [22]. Subgenus *Rigida*, composed of two–four species, is sister to the rest of the genus. The clade containing the predominantly hummock-forming subgenera *Sphagnum* and *Acutifolia* is reciprocally monophyletic to that containing the largely hollow-dwelling *Subsecunda* and *Cuspidata*, suggesting that divergence along the hydrological gradient occurred relatively early during the diversification of the genus. Most species are recognized as typically forming hummocks or growing in hollows, but some are polymorphic (e.g. *S. angustifolium* in subgenus *Cuspidata*) or cannot easily be categorized as either hummock or hollow species (e.g. species in subgenus *Rigida*).

(b) Trait quantification

Biomass decomposability was measured in a mass loss experiment conducted at McLean Bogs (Tompkins County, NY; 42.5488° N, 76.2662° W). This bog, formed following the most recent glaciation, has been used in other experiments studying peatland ecology [23,24] and is an ideal place to quantify *Sphagnum* functional traits under natural conditions. Samples of *Sphagnum*, totalling 54 species, were collected from throughout North America. Freshly collected litter was dried at room temperature and the top 5 cm of the dried plants [25,26] were placed into 5 × 5.5 cm fibre 25-micron mesh bags (Product F57, ANKOM Technology). Thirty-seven species were represented by multiple collections, and we attempted to marginalize possible intraspecific variation in litter quality by pooling an equal amount of plant material from each collection. This pooling was performed as we were interested in quantifying species mean decay rates for analysis using phylogenetic comparative methods rather than quantifying intraspecific variation *per se*. Bags were heat sealed using an impulse sealer (Product HS, ANKOM Technology), and initial mass was measured to the nearest milligram. At least 10 replicate litter bags were prepared for each species, with the exception of *S. fitzgeraldii* for which only nine were prepared due to lack of material. Litterbags were placed just beneath the surface of living *Sphagnum* in the bog for 2 years (May 2017 through May 2019). Litterbags were then air-dried for one week at room temperature. Per cent mass loss data were then used to calculate the exponential decay constant (K, yr^{-1}) for each litterbag and species means were calculated [13,27]. One litter bag for *S. torreyanum* was damaged during retrieval and was not included in the data analyses.

Quantitative data for the niche descriptor height-above-water-table (dm) were available for 34 of the 54 species sampled [28]. These niche data were used to fit evolutionary models and test for evolutionary covariance with biomass decomposability.

(c) Phylogenetic inference

Genetic data were used to reconstruct phylogeny. Sequences from six nuclear, seven plastid and two mitochondrial loci were obtained from GenBank. Nuclear loci included a ribosomal internal transcribed spacer (*ITS*), two introns in the *LEAFY*/*FLO* gene (*LL* and *LS*) and three anonymous regions (*rapdA*, *rapdB* and *rapdF*). Plastid loci included photosystem II reaction centre protein D1 (*psbA*), photosystem II reaction centre protein T (*psbT-H*), plastid ribosomal gene (*rpl16*), ribulose-bisphosphate carboxylase oxygenase large subunit (*rbcL*), ribosomal small protein 4 (*rps4*), tRNA (Gly) (UCC) (*trnG*) and the trnL (UAA) 59 exon-trnF (GAA) region (*trnL*). Mitochondrial loci include NADH dehydrogenase protein-coding subunits 5 and 7 (*nad5* and *nad7*). Multiple sequence alignment was performed using PAGAN2 v. 1.53 [29] and gap-rich regions were removed from the resulting alignments using the ‘-automated1’ heuristic algorithm in trimAl v. 1.2 [30]. The concatenated dataset was analysed with ModelFinder [31] in IQ-TREE v. 2.1.2 [32] to determine the best partitioning scheme [33] and substitution model strategy using the parameters ‘-m TESTMERGE -mset JC,HKY,GTR’ using the Bayesian information criterion.

Phylogenetic inference was performed in RevBayes v. 1.1.0 [34,35]. We estimated relative divergence times with strict molecular clocks assigned to each dataset partition. Multi-locus datasets such as this have previously been unable to confidently resolve deep nodes in the *Sphagnum* phylogeny, so we enforced a backbone constraint of subgeneric relationships, (*Rigida*,((*Sphagnum*,*Acutifolia*),(*Cuspidata*,*Subsecunda*))), to reflect the strongly supported topology recovered from analysis of nearly full mitochondrial and plastid genomes [22]. Two independent Markov chain Monte Carlo (MCMC) runs of 5E4 generations were conducted with parameters and trees sampled every five generations following a burn-in period of 1E4 generations. Each MCMC run had 23 different moves performed in a random move schedule with 186 moves per generation. The resulting samples were analysed using Tracer v. 1.7 [36] to check for stationarity and convergence on a joint posterior distribution. Finally, the tree samples from both runs were combined and summarized in a maximum *a posteriori* tree.

(d) Comparative analyses

The simplest model that we evaluated was white noise (WN) in which the species trait values are unrelated to phylogeny. The Brownian motion (BM) model incorporates species covariance and predicts increased trait variance through time at a constant rate [37]. The covariance structure for the BM model is given by the tree where the internal branch lengths are used to calculate the off-diagonal variance-covariance matrix entries; when these entries are set to zero, species’ covariances are absent and this model is equivalent to WN. The third model we considered, Lambda [38], allows for covariance entries to be less than predicted under BM but still reflect some phylogenetic signal. The Ornstein–Uhlenbeck (OU) model also allows for deviation from a pure BM model in that trait values are pulled towards some optimum value and has been described as a model of stabilizing selection [39,40].

We also evaluated other models that allowed evolutionary processes to vary across different parts of the phylogeny. Species were assigned to either ‘hummock’, ‘hollow’ or ‘polymorphic/neither’ regimes. A Mk model of evolution was used to infer ancestral states for internal nodes of the phylogeny using the ‘rerootingMethod’ function in the R package *phytools* v. 0.7-70 [41–44]. The root of the tree and the node representing the most recent common ancestor of the clade containing all subgenera except *Rigida* were assigned to the ‘polymorphic/neither’ regime as the marginal estimates provided roughly equal support for assignment to either ‘hummock’ or ‘hollow’ regimes. Variation in evolutionary rates was considered in a multi-rate BM (BMS) model, variation in adaptive optima was considered in a multi-peak OU (OUM) model, and variation in both adaptive optima and evolutionary rates was considered in a multi-rate, multi-peak OU (OUMV) model [45,46].

Evolutionary models were fitted in both maximum-likelihood and Bayesian frameworks to understand how biomass decomposability evolved during the diversification of *Sphagnum*. Maximum-likelihood analyses were implemented in the R programming environment. The WN, BM, OU and Lambda models were fitted using the package *geiger* v. 2.0.7 [47]. The BMS, OUM and OUMV models were fitted using the package *OUwie* v. 2.5 [48]. Models were compared with the Akaike information criterion (AIC) scores corrected for small sample size (AICc) and relative model likelihood was determined with Akaike weights using the package *qpcr* v. 1.4-1 [49].

Bayesian analyses were implemented in RevBayes. Model parameters were estimated using two MCMC runs of 5E4 generations, sampling every five generations and preceded by a burn-in period of 1E4 generations. The resulting samples were analysed using Tracer v. 1.7 [36] to check for stationarity and convergence on a joint posterior distribution. The marginal likelihood of each model was estimated using the stepping-stone power posterior method with 1E2 stones traversing the posterior and prior distributions [50]. These marginal-likelihood estimates (mL) were used to compare models using both Bayes factors and relative model probability calculated from the following equation:

$$P(\text{Model}) = \frac{mL_{\text{Model}}}{\sum_i \text{mL}_i} = \frac{\mathrm{e}^{(\ln mL_{\text{Model}} - \ln mL_{\text{Max}})}}{\sum_i \mathrm{e}^{(\ln mL_i - \ln mL_{\text{Max}})}}.$$

All evolutionary models were fitted using the average decay constant (K, yr^{-1}) across replicate litter bags for each species and the maximum *a posteriori* tree. We considered the variance and standard error for Bayesian and likelihood analyses, respectively, as intraspecific variation and measurement error can affect such modelling substantially [51]. Finally, we fitted these models in a likelihood framework using a randomly selected subset of 1E3 trees from the posterior tree distribution to account for phylogenetic uncertainty.

We fit a reversible-jump MCMC (rjMCMC) model to allow the data to determine the most probable location of selective regime shifts on the phylogeny in the model fitting multiple adaptive optima (i.e. OUM) rather than providing *a priori* regime assignment. In this model, each branch had an equal probability for such a regime shift in decomposability (K, yr^{-1}). The model parameters were estimated using two MCMC runs of 5E4 generations, sampling every five generations and preceded by a burn-in period of 1E4 generations. We visualized the results of the rjMCMC model using the R package *RevGadgets* v. 1.0.0 [52].

Finally, we tested for evolutionary covariance of biomass decomposability and the niche descriptor height-above-water-table. First, tips in the maximum *a posteriori* tree that did not have niche descriptor data were pruned using the R package *ape* v. 5.4-1 [53]. Next, all evolutionary models were fitted using the niche descriptor data. Finally, a phylogenetic generalized least-squares (PGLS) model was fitted using the R package *caper* v. 1.0.1 [54] to determine if decomposability was a significant predictor of niche. PGLS was performed as the residual errors of an ordinary least-squares regression model had phylogenetic signal indicated by comparison of AICc values among BM, WN and Lambda models and significant one-tailed likelihood ratio tests of both BM and Lambda models against the WN model (BM: $\text{LR} = 7.2$, $\text{d.f.} = 1$, $p = 7.4 \times 10^{-3}$; Lambda: $\text{LR} = 7.2$, $\text{d.f.} = 2$, $p = 2.8 \times 10^{-2}$).

Information about the choice of priors for Bayesian analyses can be found in the electronic supplementary material, tables S1–S3.

(e) Other statistical analyses

We fitted phylogenetic linear mixed-effects models in R using restricted maximum likelihood with the package *phyr* v. 1.1.0 [55] to determine if the fixed effect of the microhabitat regime was a significant predictor of biomass decomposability. The data were analysed unaggregated, and we treated species identity as a random effect. To account for phylogeny, we used the maximum *a posteriori* tree to estimate the correlation structure among species. Residuals were visually inspected for normality, and Levene’s test [56] was used to test for homogeneity of variance using the R package *car* v. 3.0-10 [57]. Likelihood ratio tests were performed to conduct hypothesis testing. Data were log-transformed, and outliers were removed to meet assumptions

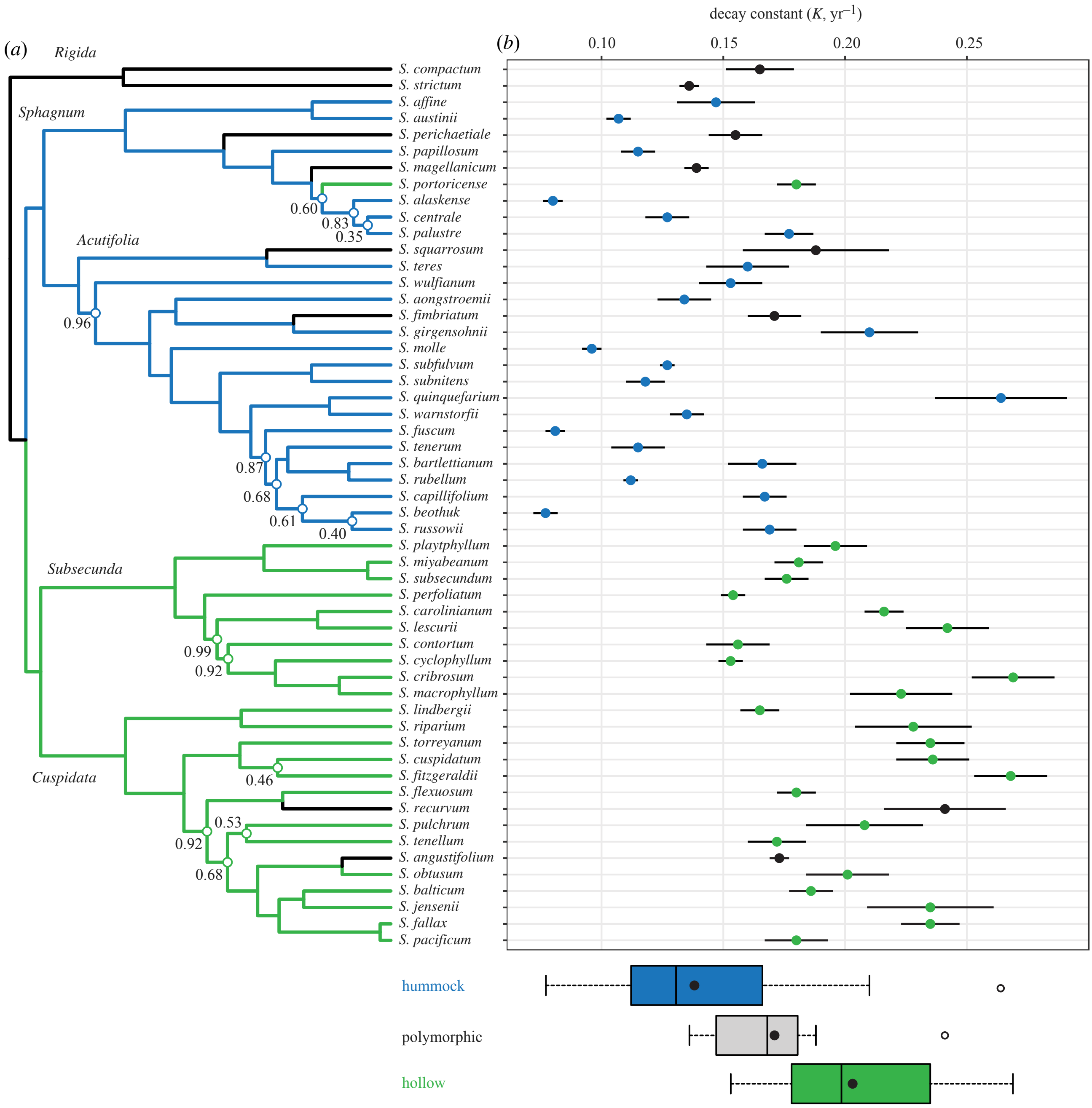

Figure 1. Phylogenetic relationships and trait data for 54 peat moss species suggest that interspecific variation in litter decomposability relates to the phylogeny of *Sphagnum*. (*a*) The Bayesian maximum *a posteriori* tree depicting evolutionary relationships with labelled bipartitions receiving support less than 1.0 posterior probability. (*b*) Species mean decay constant (K, yr^{-1}) ± s.e.m. Colour indicates microhabitat preference for hummock (blue), hollow (green) or polymorphic (black) species. Box plots depict the medians (centre lines), means (closed circles), upper/lower quartiles (box limits), 1.5 x interquartile ranges (whiskers) and outliers (open circles). (Online version in colour.)

of the model. Analysis using the raw data, although violating some assumptions of the model, still recovers a significant effect of microhabitat regime albeit at a higher significance level (LR = 7.9, d.f. = 2, $p = 1.9 \times 10^{-2}$).

3. Results

Reconstructed evolutionary relationships among *Sphagnum* species suggest that interspecific variation in biomass decomposability is related to the peat moss phylogeny. Mean species decomposability (K, yr^{-1}) ranges from 0.153 to 0.269 in hollow lineages, from 0.077 to 0.264 in hummock lineages, and from 0.136 to 0.241 in polymorphic lineages. When values for species mean decomposability are mapped onto the tree, it is evident that species in the largely hummock-forming clade, containing subgenera *Sphagnum* and *Acutifolia*, have lower decomposability than species in the largely hollow clade, containing subgenera *Subsecunda* and *Cuspidata* (figure 1). Analysis using phylogenetic linear mixed models indicates a significant effect of habitat regime on decomposability (LR = 19.1, d.f. = 2, $p = 7.2 \times 10^{-5}$), suggesting that litter produced by hummock-forming species decays more slowly than hollow-dwelling species. While the backbone relationships among subgenera were constrained to those reconstructed using organellar genome sequences, we found that evolutionary relationships within subgenera are largely well-supported with the majority of bipartitions having greater than 0.95 posterior probability in each subgenus: *Sphagnum* (approx. 57%), *Acutifolia* (75%), *Subsecunda* (approx. 88%) and *Cuspidata* (approx. 69%). However, some regions of the phylogeny, such as those

Table 1. Comparison of evolutionary models indicates the presence of adaptive trait optima for litter decomposability (K, yr^{-1}) in *Sphagnum*. Model abbreviations and brief descriptions are provided. For maximum-likelihood results, delta AICc (ΔAIC_c) values and corresponding AICc weights (W_i) are provided for each model. For Bayesian results, the Bayes factor relative to the model with the largest marginal-likelihood estimate (2ln(BF)) and corresponding model probability (P(Model)) is provided.

			likelihood		Bayesian	
model	**abbr.**	**description**	**ΔAIC_c**	**W_i**	**2ln(BF)**	**P(model)**
white noise	WN	trait variance increases over time with no phylogenetic signal	19.46	0.00	32.81	0.00
Brownian motion	BM	trait variance increases over time with phylogenetic signal	32.00	0.00	40.47	0.00
Lambda	Lambda	trait variance increases over time with phylogenetic signal that can be weaker than BM	8.91	0.01	38.64	0.00
Ornstein–Uhlenbeck	OU	trait variance increases over time with phylogenetic signal trait values are pulled towards some optimum value	17.38	0.00	21.26	0.00
multi-rate Brownian motion	BMS	trait variance increases over time with phylogenetic signal regimes have separate evolutionary rates	29.71	0.00	45.76	0.00
multi-peak Ornstein–Uhlenbeck	OUM	trait variance increases over time with phylogenetic signal regimes have separate adaptive optima	0.00	0.83	0.00	0.79
multi-peak, multi-rate Ornstein–Uhlenbeck	OUMV	trait variance increases over time with phylogenetic signal regimes have separate evolutionary rates and adaptive optima	3.25	0.16	2.68	0.21

relationships among species in the *S. capillifolium* complex, were not confidently resolved. Nevertheless, this phylogenetic uncertainty was accounted for in our analysis as models of trait evolution were fitted with 1000 different trees from the Bayesian posterior tree distribution.

Using the phylogeny and trait data, we competed seven models to better characterize the mode and tempo of evolution in *Sphagnum* biomass decomposability (table 1). Models that incorporate natural selection and predict separate trait optima for litter decomposability among microhabitat regimes outperform all other models that do not include such optima. The model that best describes the evolution of biomass decomposability is a multi-peak Ornstein–Uhlenbeck process (OUM), wherein there exist separate optima toward which stabilizing selection pulls trait values (figure 2). In our maximum-likelihood analyses, the OUM model has the lowest corrected Akaike information criterion (AICc) score and the majority of the AICc weight (table 1). The OUM model maximum-likelihood estimate for optimum biomass decomposability (K, yr^{-1}) in the hummock selective regime is 0.138 ± 0.008, while that in the hollow regime is 0.204 ± 0.008 and that in the polymorphic regime is 0.171 ± 0.015. The model incorporating separate trait optima and evolutionary rates among regimes (OUMV) also performs well, receiving substantial evidence based on AICc scores and nearly all of the remaining AICc weight. Similar results are obtained from Bayesian model selection, where the OUM model has the highest marginal-likelihood and model probability. Our findings are robust when measurement error is considered in model fitting (electronic supplementary material, table S4). Additionally, the results are robust to phylogenetic uncertainty in maximum-likelihood analyses with OUM as the best model for 98.6% of 1000 trees from the posterior distribution and the Lambda model preferred for 1.4% of trees (electronic supplementary material, table S5). Additional analyses that did not require *a priori* hypotheses about the location of possible shifts in adaptive optima for decomposability support the finding of selective regime divergence early during *Sphagnum* diversification, with different hummock and hollow selective regimes recovered at 0.94 posterior probability (figure 2).

We also found that the divergence of optimum decomposability in the ancestors of the crown groups within *Sphagnum* resulted in separate optimum niches to which species are adapted. Our analyses show that the position of species along the microtopographic gradient height-above-water-table is not only phylogenetically conserved but that the predominantly hummock and hollow clades of *Sphagnum* have separate adaptive optima for realized niche (electronic supplementary material, table S6). Using likelihood, we are unable to confidently fit models that incorporate separate

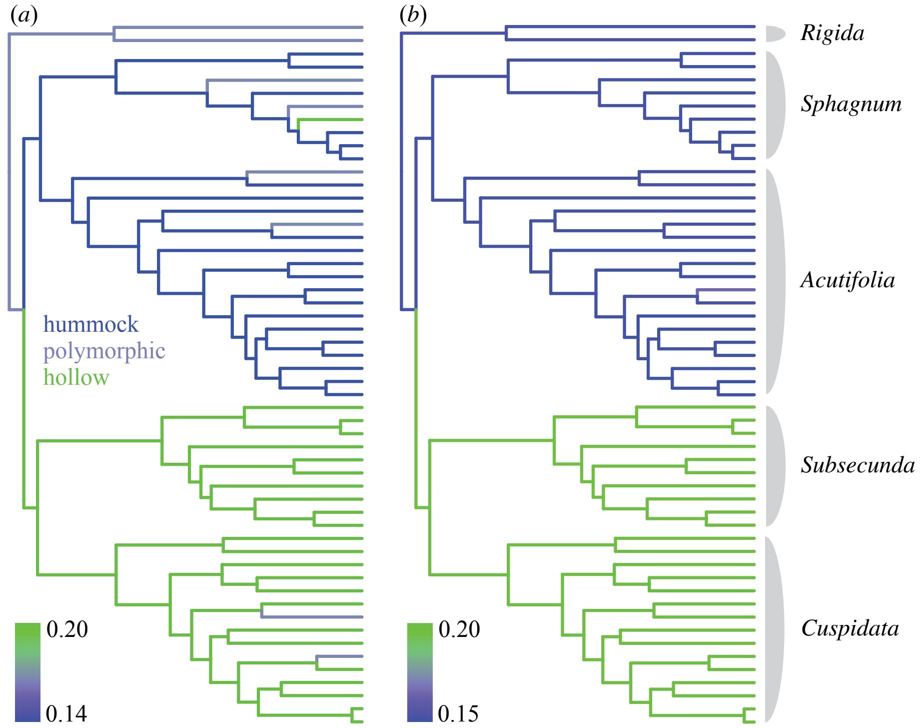

Figure 2. Adaptive optima for litter decomposability (K, yr^{-1}) in the genus *Sphagnum*. (*a*) We found support for the hypothesis that species in hummock (blue), hollow (green) and polymorphic (teal) regimes have separate optima towards which trait values are pulled. (*b*) Bayesian reversible-jump MCMC analysis suggests a shift from lower (blue) to higher (green) optimum decay constant occurred in the ancestor to the clade containing subgenera *Subsecunda* and *Cuspidata* at 0.94 posterior probability. (Online version in colour.)

rates of evolution for each regime due to the presence of saddle points. These saddle points also exist when fitting the decomposability data using only the 34 species for which height-above-water-table data are available suggesting that our inability to fit these models stems from a lack of statistical power. Nevertheless, the OUM model best describes the evolution of height-above-water-table in a likelihood framework and is nearly indistinguishable from the preferred OUMV model in our Bayesian analyses. These models suggest that the hummock species have a higher adaptive optimum for height-above-water-table than species in the hollow or polymorphic regimes and that shifts in this optima occurred concomitantly with corresponding decreases in biomass decomposability (figure 3). Finally, PGLS regression indicates that decomposability under natural conditions is a significant predictor of species niche ($F(1,32) = 9.8$, $p = 3.8 \times 10^{-3}$, adjusted $R^2 = 0.21$; figure 4).

4. Discussion

The evolution of *Sphagnum* biomass decomposability is a result of natural selection and divergence in trait optima among species with different niches occurred prior to the diversification of the genus. We found that variation in decomposability under natural conditions and niche preference along with height-above-water-table track phylogenetic relationships in *Sphagnum*. Moreover, we found that the coevolution of decomposability and niche is driven by selection and not merely a consequence of random evolutionary walks. Therefore, the construction of boreal peatlands, and the microhabitat niches therein, via *Sphagnum* decomposability highlights the importance of this specific functional trait to carbon cycling at an ecosystem scale. Perhaps too often, the term ‘ecosystem engineering’ is applied to environmental changes that are not at the ecosystem scale *per se*. Nevertheless, our findings in *Sphagnum* represent a unique case of natural selection shaping the evolution of ecosystem engineering through phenotypes that extend beyond the plants themselves.

Both our maximum-likelihood and Bayesian analyses provided support for the hypothesis that hummock species have less biomass decomposability than hollow species due to a shift in the selective regime. The differences between adaptive optima for biomass decomposability may seem small, but the predicted consequences over time are dramatic: litter produced from hummock species is predicted to take over a year longer to lose half of its initial biomass when compared to that produced by hollow species. The presence of adaptive optima among clades of *Sphagnum* for litter decomposability parallels recent findings in flowering plants and suggests that selection might act on this functional trait throughout the land plant phylogeny [58,59], perhaps in part due to pleiotropic effects on other functional traits such as growth or secondary metabolism.

Evolutionary rate estimates in the OUMV model indicate that decomposability evolves faster in hummock lineages, which likely reflects the slightly larger variance of decay constant values among species and greater homoplasy in niche preference within the predominantly hummock-forming subgenera *Sphagnum* and *Acutifolia*. For example, *S. portoricense*, in the typically hummock-forming subgenus *Sphagnum*, is a largely tropical species that grows close to the water table and has a much higher biomass decomposability than the related *S. alaskense* that forms moderately sized hummocks. Similar results were obtained from fitting the OUMV model

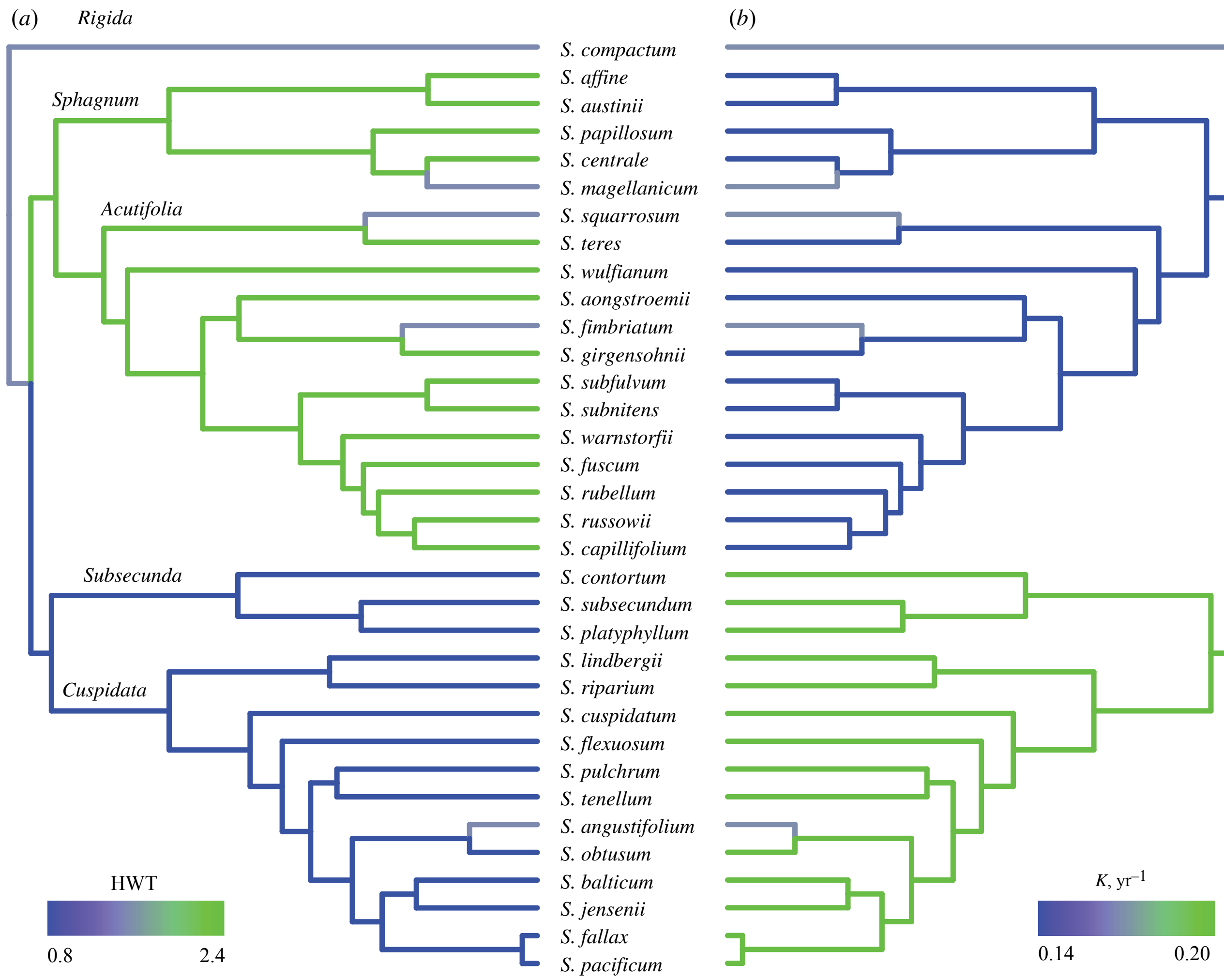

Figure 3. The adaptive optima for biomass decomposability (K, yr^{-1}) have corresponding optima in a realized niche along the height-above-water-table (dm) microhabitat gradient. (*a*) Species in the hummock regime have higher (green) optimum height-above-water-table than do species in polymorphic or hollow regimes. (*b*) Species in the hummock regime have lower (blue) optimum decomposability than do species in polymorphic or hollow regimes. (Online version in colour.)

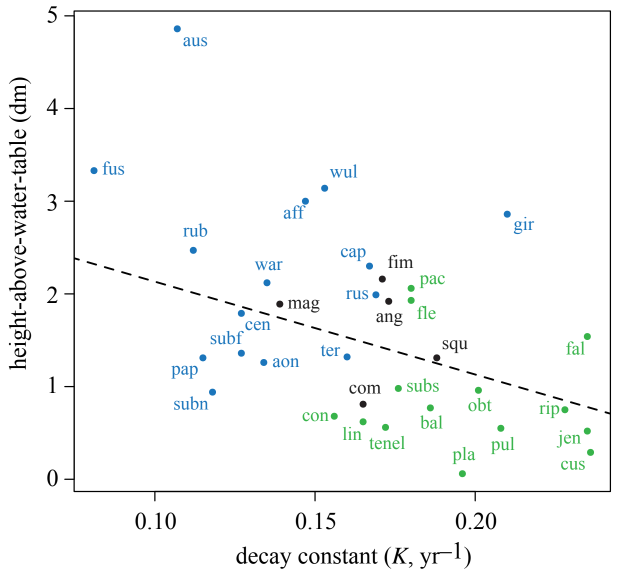

Figure 4. Biomass decomposability (K, yr^{-1}) is negatively correlated with the hydrological height-above-water-table (dm) gradient. Hummock species (blue dots) tend to grow higher above the water table and have lower decomposability as compared to hollow species (green dots) and polymorphic species (black dots). PGLS regression: $F(1,32) = 9.8$, $p = 3.8 \times 10^{-3}$ and adjusted $R^2 = 0.21$. (Online version in colour.)

to the quantitative height-above-water-table data in a Bayesian framework and under likelihood using standard error, suggesting that the increased rate of evolution in decomposability within predominantly hummock-forming clades is recapitulated by an increased rate of evolution in a realized niche.

Phylogenetic conservatism of biomass decomposability suggests a strong genetic basis for this trait and, combined with the finding that natural selection shapes trait variation in *Sphagnum*, represents a fascinating model of the 'extended phenotype' where genetic variation produces variation in organismal artefacts, which create the environmental conditions that, in turn, select across levels of biological organization [60,61]. It must be acknowledged that the quality of the initial plant litter can be influenced by environmental conditions and, while we attempted to marginalize such effects in our experiment, future studies might improve upon this work by quantifying intraspecific variation explicitly and addressing the relative importance of genotype, environment and genotype-by-environment interaction in determining litter decomposability. With emerging genomic resources for *Sphagnum* generated by a genus-wide sequencing project [62], these findings set the stage for elucidating the specific genomic targets of selection that underlie the evolution of adaptive trait syndromes associated with hummock and hollow niches. Additionally, such an increase in our understanding of how peat moss species differ in functional traits can help better inform ecological models of nutrient flux both globally and within peatlands, better forecast the fate of peat carbon stocks and improve predictions of how community structure within peatland ecosystems might respond as Earth's climate rapidly changes.

Data accessibility. All data and code used in the analysis can be accessed at Figshare (doi:10.6084/m9.figshare.14109725). The voucher specimens for collections are stored in the Duke Bryophyte Herbarium (DUKE).

Authors' contributions. B.T.P.: conceptualization, data curation, formal analysis, funding acquisition, investigation, methodology, resources, software, visualization, writing-original draft, writing-review and editing; J.B.Y.: investigation, methodology, resources, writing-review and editing; M.R.T.: investigation, methodology, resources, writing-review and editing; A.J.S.: conceptualization, funding acquisition, methodology, project administration, resources, supervision, writing-review and editing.

All authors gave final approval for publication and agreed to be held accountable for the work performed therein.

Competing interests. The authors declare no competing interests.

Funding. This work was supported by funding from the Duke University Graduate School, the North Carolina Native Plant Society and the US National Science Foundation (grant no. DEB-1737899).

Acknowledgements. We thank R. S. Clymo and the reviewers for suggesting improvements on previous versions of this manuscript. We thank Steve Rice and the late Dick Andrus for their assistance in performing fieldwork. We thank Cornell University for access to the McLean Bogs field site and permission to conduct the experiment.

References

1. Gorham E. 1991 Northern peatlands: role in the carbon cycle and probable responses to climatic warming. *Ecol. Appl.* **1**, 182–195. (doi:10.2307/1941811)
2. Jones CG, Lawton JH, Shachak M. 1994 Organisms as ecosystem engineers. *Oikos* **69**, 373–386. (doi:10.2307/3545850)
3. Yu Z. 2012 Northern peatland carbon stocks and dynamics: a review. *Biogeosciences* **9**, 4071–4085. (doi:10.5194/bg-9-4071-2012)
4. Clymo RS, Hayward PM. 1982 The ecology of *Sphagnum*. In *Bryophyte ecology* (ed. AJE Smith), pp. 229–289. London, UK: Chapman and Hall.
5. Shaw AJ, Devos N, Cox CJ, Boles SB, Shaw B, Buchanan AM, Cave L, Seppelt R. 2010 Peatmoss (*Sphagnum*) diversification associated with Miocene Northern Hemisphere climatic cooling? *Mol. Phylogenet. Evol.* **55**, 1139–1145. (doi:10.1016/j.ympev.2010.01.020)
6. Van Breemen N. 1995 How *Sphagnum* bogs down other plants. *Trends Ecol. Evol.* **10**, 270–275. (doi:10.1016/0169-5347(95)90007-1)
7. Aerts R, Verhoeven JTA, Whigham DF. 1999 Plant-mediated controls on nutrient cycling in temperate fens and bogs. *Ecology* **80**, 2170–2181. (doi:10.1890/0012-9658(1999)080[2170:PMCONC]2.0.CO;2)
8. Vitt DH, Slack NG. 1984 Niche diversification of *Sphagnum* relative to environmental factors in northern Minnesota peatlands. *Can. J. Bot.* **62**, 1409–1430. (doi:10.1139/b84-192)
9. Pouliot R, Rochefort L, Karofeld E. 2011 Initiation of microtopography in revegetated cutover peatlands. *Appl. Veg. Sci.* **14**, 158–171. (doi:10.1111/j.1654-109X.2010.01118.x)
10. Johnson LC, Damman AWH. 1991 Species-controlled *Sphagnum* decay on a South Swedish raised bog. *Oikos* **61**, 234–242. (doi:10.2307/3545341)
11. Hájek T. 2009 Habitat and species controls on *Sphagnum* production and decomposition in a mountain raised bog. *Boreal Environ. Res.* **14**, 947–958.
12. Belyea LR. 1996 Separating the effects of litter quality and microenvironment on decomposition rates in a patterned peatland. *Oikos* **77**, 529–539. (doi:10.2307/3545942)
13. Turetsky MR, Crow SE, Evans RJ, Vitt DH, Wieder RK. 2008 Trade-offs in resource allocation among moss species control decomposition in boreal peatlands. *J. Ecol.* **96**, 1297–1305. (doi:10.1111/j.1365-2745.2008.01438.x)
14. Bengtsson F, Granath G, Rydin H. 2016 Photosynthesis, growth, and decay traits in *Sphagnum*—a multispecies comparison. *Ecol. Evol.* **6**, 3325–3341. (doi:10.1002/ece3.2119)
15. Limpens J, Bohlin E, Nilsson MB. 2017 Phylogenetic or environmental control on the elemental and organo-chemical composition of *Sphagnum* mosses? *Plant Soil* **417**, 69–85. (doi:10.1007/s11104-017-3239-4)
16. Bengtsson F, Rydin H, Hájek T. 2018 Biochemical determinants of litter quality in 15 species of *Sphagnum*. *Plant Soil* **425**, 161–176. (doi:10.1007/s11104-018-3579-8)
17. Chiapusio G, Jassey VEJ, Bellvert F, Comte G, Weston LA, Delarue F, Buttler A, Toussaint ML, Binet P. 2018 *Sphagnum* species module their phenolic profiles and mycorrhizal colonization of surrounding *Andromeda polifolia* along peatland microhabitats. *J. Chem. Ecol.* **44**, 1146–1157. (doi:10.1007/s10886-018-1023-4)
18. Johnson MG, Granath G, Tahvanainen T, Pouliot R, Stenøien HK, Rochefort L, Rydin H, Shaw AJ. 2015 Evolution of niche preference in *Sphagnum* peat mosses. *Evolution* **69**, 90–103. (doi:10.1111/evo.12547)
19. Piatkowski BT, Shaw AJ. 2019 Functional trait evolution in *Sphagnum* peat mosses and its relationship to niche construction. *New Phytol.* **223**, 939–949. (doi:10.1111/nph.15825)
20. Price PW. 1994 Phylogenetic constraints, adaptive syndromes, and emergent properties: from individuals to population dynamics. *Res. Popul. Ecol.* **36**, 3–14. (doi:10.1007/BF02515079)
21. Barrett SCH. 2010 Understanding plant reproductive diversity. *Phil. Trans. R. Soc. Lond. B* **365**, 99–109. (doi:10.1098/rstb.2009.0199)
22. Shaw AJ, Devos N, Liu Y, Cox CJ, Goffinet B, Flatberg KI, Shaw B. 2016 Organellar phylogenomics of an emerging model system: *Sphagnum* (peatmoss). *Ann. Bot.* **118**, 185–196. (doi:10.1093/aob/mcw086)
23. Osvald H. 1970 Vegetation and stratigraphy of peatlands in North America. *Nova Acta Regiae Societatis Scientarium Upsaliensis Series V: C* **1**, 1–96.
24. Williams CJ, Shingara EA, Yavitt JB. 2000 Phenol oxidase activity in peatlands in New York State: response to summer drought and peat type. *Wetlands* **20**, 416–421. (doi:10.1672/0277-5212(2000)020[0416:POAIPI]2.0.CO;2)
25. Coulson JC, Butterfield J. 1978 An investigation of the biotic factors determining the rates of plant decomposition on blanket bog. *J. Ecol.* **66**, 631–650. (doi:10.2307/2259155)
26. Thormann MN, Bayley SE, Currah RS. 2001 Comparison of decomposition of belowground and aboveground plant litters in peatlands of boreal Alberta, Canada. *Can. J. Bot.* **79**, 9–22. (doi:10.1139/b00-138)
27. Olson JS. 1963 Energy storage and the balance of producers and decomposers in ecological systems. *Ecology* **44**, 322–331. (doi:10.2307/1932179)
28. Johnson MG, Granath G, Tahvanainen T, Pouliot R, Stenøien HK, Rochefort L, Rydin H, Shaw AJ. 2015 Data from: Evolution of niche preference in *Sphagnum* peat mosses. See https://onlinelibrary.wiley.com/action/downloadSupplement?doi=10.1111%2Fevo.12547&file=evo12547-sup-0001-SuppMat.docx.
29. Löytynoja A, Vilella AJ, Goldman N. 2012 Accurate extension of multiple sequence alignments using a phylogeny-aware graph algorithm. *Bioinform* **13**, 1683–1691. (doi:10.1093/bioinformatics/bts198)
30. Capella-Gutiérrez S, Silla-Martínez JM, Gabaldón T. 2009 trimAl: a tool for automated alignment trimming in large-scale phylogenetic analyses. *Bioinform* **25**, 1972–1973. (doi:10.1093/bioinformatics/btp348)
31. Kalyaanamoorthy S, Minh BQ, Wong TKF, Von Haeseler A, Jermiin LS. 2017 ModelFinder: fast model selection for accurate phylogenetic estimates. *Nat. Methods* **14**, 587–589. (doi:10.1038/nmeth.4285)

32. Minh BQ, Schmidt HA, Chernomor O, Schrempf D, Woodhams MD, Von Haeseler A, Teeling E. 2020 IQ-TREE 2: new models and efficient methods for phylogenetic inference in the genomic era. *Mol. Biol. Evol.* **37**, 1530–1534. (doi:10.1093/molbev/msaa015)
33. Chernomor O, Von Haeseler A, Minh BQ. 2016 Terrace aware data structure for phylogenomic inference from supermatrices. *Syst. Biol.* **67**, 997–1008. (doi:10.1093/sysbio/syw037)
34. Höhna S, Heath TA, Boussau B, Landis MJ, Ronquist F, Huelsenbeck JP. 2014 Probabilistic graphical model representation in phylogenetics. *Syst. Biol.* **63**, 753–771. (doi:10.1093/sysbio/syu039)
35. Höhna S, Landis MJ, Heath TA, Boussau B, Lartillot N, Moore BR, Huelsenbeck JP, Ronquist F. 2016 RevBayes: Bayesian phylogenetic inference using graphical models and an interactive model-specification language. *Syst. Biol.* **65**, 726–736. (doi:10.1093/sysbio/syw021)
36. Rambaut A, Drummond AJ, Xie D, Baele G, Suchard MA. 2018 Posterior summarization in Bayesian phylogenetics using Tracer 1.7. *Syst. Biol.* **67**, 901–904. (doi:10.1093/sysbio/syy032)
37. Felsenstein J. 1985 Phylogenies and the comparative method. *Am. Nat.* **125**, 1–15. (doi:10.1086/284325)
38. Pagel M. 1999 Inferring the historical patterns of biological evolution. *Nature* **401**, 877–884. (doi:10.1038/44766)
39. Hansen TF. 1997 Stabilizing selection and the comparative analysis of adaptation. *Evolution* **51**, 1341–1351. (doi:10.1111/j.1558-5646.1997.tb01457.x)
40. Butler MA, King AA. 2004 Phylogenetic comparative analysis: a modeling approach for adaptive evolution. *Am. Nat.* **164**, 683–695. (doi:10.1086/426002)
41. Yang Z, Kumar S, Nei M. 1995 A new method of inference of ancestral nucleotide and amino acid sequences. *Genetics* **141**, 1641–1650. (doi:10.1093/genetics/141.4.1641)
42. Lewis PO. 2001 A likelihood approach to estimating phylogeny from discrete morphological character data. *Syst. Biol.* **6**, 913–925. (doi:10.1080/106351501753462876)
43. Revell LJ. 2012 phytools: an R package for phylogenetic comparative biology (and other things). *Methods Ecol. Evol.* **3**, 217–223. (doi:10.1111/j.2041-210X.2011.00169.x)
44. Core Team R. 2020 *R: a language and environment for statistical computing. Version 4.0.3*. Vienna, Austria: R Foundation for Statistical Computing. See https://www.R-project.org/.
45. O'Meara BC, Ané C, Sanderson MJ, Wainwright PC. 2006 Testing for different rates of continuous trait evolution using likelihood. *Evolution* **60**, 922–933. (doi:10.1111/j.0014-3820.2006.tb01171.x)
46. Beaulieu JM, Jhwueng D-C, Boettiger C, O'meara BC. 2012 Modeling stabilizing selection: expanding the Ornstein-Uhlenbeck model of adaptive evolution. *Evolution* **66**, 2369–2383. (doi:10.1111/j.1558-5646.2012.01619.x)
47. Pennell MW, Eastman JM, Slater GJ, Brown JW, Uyeda JC, Fitzjohn RG, Alfaro ME, Harmon LJ. 2014 Geiger v2.0: an expanded suite of methods for fitting macroevolutionary models to phylogenetic trees. *Bioinform* **30**, 2216–2218. (doi:10.1093/bioinformatics/btu181)
48. Beaulieu JM, O'meara B. 2019 OUwie: analysis of evolutionary rates in an OU framework. R package version 1.57. See https://CRAN.R-project.org/package=OUwie.
49. Spiess A-N. 2018 qpcR: modelling and analysis of real-time PCR data. R package version 1.4-1. See https://CRAN.R-project.org/package=qpcR.
50. Xie W, Lewis PO, Fan Y, Kuo L, Chen MH. 2011 Improving marginal likelihood estimation for Bayesian phylogenetic model selection. *Syst. Biol.* **60**, 150–160. (doi:10.1093/sysbio/syq085)
51. Ives AR, Midford PE, Garland Jr T. 2007 Within-species variation and measurement error in phylogenetic comparative methods. *Syst. Biol.* **56**, 252–270. (doi:10.1080/10635150701313830)
52. Höhna S, Freyman WA. 2016 RevGadgets: process output generated by RevBayes. R package version 1.0.0. See https://github.com/revbayes/RevGadgets.
53. Paradis E, Schliep K. 2018 ape 5.0: an environment for modern phylogenetics and evolutionary analyses in R. *Bioinform* **35**, 526–528. (doi:10.1093/bioinformatics/bty633)
54. Orme D, Freckleton R, Thomas G, Petzoldt T, Fritz S, Isaac N. 2018 caper: comparative analyses of phylogenetics and evolution in R. R package version 1.0.1. See https://CRAN.R-project.org/package=caper.
55. Li D, Dinnage R, Nell NA, Helmus MR, Ives AR. 2020 phyr: an R package for phylogenetic species-distribution modelling in ecological communities. *Methods Ecol. Evol.* **11**, 1455–1463. (doi:10.1111/2041-210X.13471)
56. Levene H. 1960 Robust tests for equality of variances. In *Contributions to probability and statistics: essays in Honor of Harold Hotelling* (eds I Olkin, H Hotelling), pp. 278–292. Palo Alto, CA: Stanford University Press.
57. Fox J, Weisberg S. 2019 *An R companion to applied regression*, 3rd edn. Thousand Oaks, CA: Sage.
58. Pan X, Cornelissen JHC, Zhao WW, Liu GF, Hu YK, Prinzing A, Dong M, Cornwell WK. 2014 Experimental evidence that the Ornstein-Uhlenbeck model best describes the evolution of leaf litter decomposability. *Ecol. Evol.* **4**, 3339–3349. (doi:10.1002/ece3.1115)
59. Leroy CJ *et al.* 2020 Plant phylogenetic history explains in-stream decomposition at a global scale. *J. Ecol.* **108**, 17–35. (doi:10.1111/1365-2745.13262)
60. Dawkins R. 1982 *The extended phenotype: the long reach of the gene*, pp. 195–208. Oxford, UK: Oxford University Press.
61. Laland K, Matthews B, Feldman MW. 2016 An introduction to niche construction theory. *Evol. Ecol.* **30**, 191–202. (doi:10.1007/s10682-016-9821-z)
62. Weston DJ *et al.* 2018 The Sphagnome Project: enabling ecological and evolutionary insights through a genus-level sequencing project. *New Phytol.* **217**, 16–25. (doi:10.1111/nph.14860)